Human Coronavirus OC43 Nucleocapsid Protein Binds MicroRNA 9 and Potentiates NF-κB Activation

Frances W. Lai,[a,b] Kyle B. Stephenson,[a]* James Mahony,[b,c] Brian D. Lichty[a,b]

McMaster Immunology Research Centre, Department of Pathology & Molecular Medicine, McMaster University, Hamilton, Ontario, Canada[a]; MG DeGroote Institute for Infectious Disease Research, McMaster University, Hamilton, Ontario, Canada[b]; St. Joseph's Healthcare, Hamilton, Ontario, Canada[c]

The human coronavirus OC43 is a major contributor to the common cold worldwide, though due to its low mortality rate, little research has focused on this human pathogen. The nucleocapsid is an essential structural protein with conserved functions across the coronavirus family. While a multitude of studies have examined nucleocapsid function, none have described the effects of OC43 nucleocapsid on the transcription factor NF-κB. We report that the nucleocapsid protein of OC43 causes potentiation of NF-κB activation. This prolonged activation is the direct result of the ability of the nucleocapsid to bind RNA, specifically microRNA 9 (miR-9), which is a negative regulator of NF-κB. This previously undescribed interaction between virus and host is a potential mechanism of immune evasion in RNA viruses.

Coronaviruses (CoV) are large, enveloped, positive-stranded RNA viruses classified in the order *Nidovirales* that infect humans as well as a vast array of animals. Human coronaviruses (HCoV), such as prototypic virus OC43, have not been well studied, but the emergence of severe acute respiratory syndrome-related coronavirus (SARS-CoV) in 2002 spurred new interest in HCoV over the last decade (1). The HCoV OC43 was isolated from patients in the 1960s who had symptoms of the common cold (2). Along with being a major cause of the common cold, OC43 also causes pneumonia in the immunocompromised, with several outbreaks in the elderly underscoring the morbidity and mortality caused by this virus (3–5).

The nucleocapsid protein (N) of coronaviruses is essential to replication and binds genomic RNA to form a helical capsid. As RNA viruses do, CoV replicate solely in the cytoplasm, but the N protein is not restricted to this site, as the N protein of multiple coronaviruses and related nidoviruses have been found to localize to the nucleus and nucleolus, with the function of this shuttling remaining unknown, though it has been speculated to disrupt cell growth (6–9). It is known that N is generally a multifunctional protein, as it has been found to be an RNA chaperone and interact with cellular proteins cyclophilin A, Smad3, B23, and nucleolar proteins fibrillarin and nucleolin, both key proteins in ribosome biogenesis and nucleolar assembly (9–13).

With the manifestation of SARS-CoV, interest has increased exponentially in HCoV; however, few studies have been conducted on the innate immune response, particularly the activation of NF-κB, during other HCoV infections. The effect of SARS-CoV N on NF-κB has been examined with conflicting results. There have been studies that state SARS-CoV N activates NF-κB (14, 15), and one that states N inhibits NF-κB activation (16). There have been no published studies examining the effect of OC43 N on NF-κB to date.

NF-κB is a multifunctional transcription factor that is prominent in the innate immune response to virus infection. It is activated via many stimuli and signals through pathways, including tumor necrosis factor alpha (TNF-α), interleukin 1 (IL-1), and Toll-like receptor (TLR) ligands, such as double-stranded RNA and lipopolysaccharide (LPS) (reviewed in reference 17). There are five mammalian members of the NF-κB family: RelA (p65), RelB, c-Rel, p105/p50, and p100/p52. These transcription factors regulate the expression of many genes involved in inflammation, apoptosis, and the innate immune response (reviewed in reference 18). p65, RelB, and c-Rel contain transactivation domains (TADs), and dimers of these subunits are traditionally known as transcriptional activators which are retained in the cytoplasm by inhibitory IκB proteins in unstimulated cells. In contrast, both p105 and p100 lack TADs and are precursors to the subunits p50 and p52, respectively. The 20S proteasomal processing of p105 to p50 can occur cotranslationally or independently of translation (19, 20). In an unstimulated cell, p50 forms homodimers which act as transcriptional repressors complexed with transcriptional corepressors, such as histone deacetylase 3 (HDAC3) and silencing mediator of retinoic acid and thyroid hormone receptor (SMRT) (21). Homodimers of p50 have also been found to be transcriptionally active when complexed with atypical IκB proteins, such as IκBζ and BCL-3, resulting in upregulation of anti-inflammatory cytokine IL-10 (22, 23). The p50 subunit can also form dimers with p65 and transcriptional coactivators such as CREB-binding protein (CBP) (24). Once the cell has been stimulated, resulting in activation of its IκB kinase (IKK) complex, these NF-κB heterodimers compete with p50 homodimers for κB site binding.

The expression and transcriptional activation of NF-κB are tightly regulated. The expression of many negative regulators of NF-κB, such as A20 and IκBα, is induced by activation of NF-κB itself (25). Recently, another mechanism of control was found to negatively regulate the expression of *NFKB1*, which encodes p105. microRNA 9 (miR-9) was shown to target the 3′ untranslated region (3′UTR) of *NFKB1* and resulted in decreased mRNA ex-
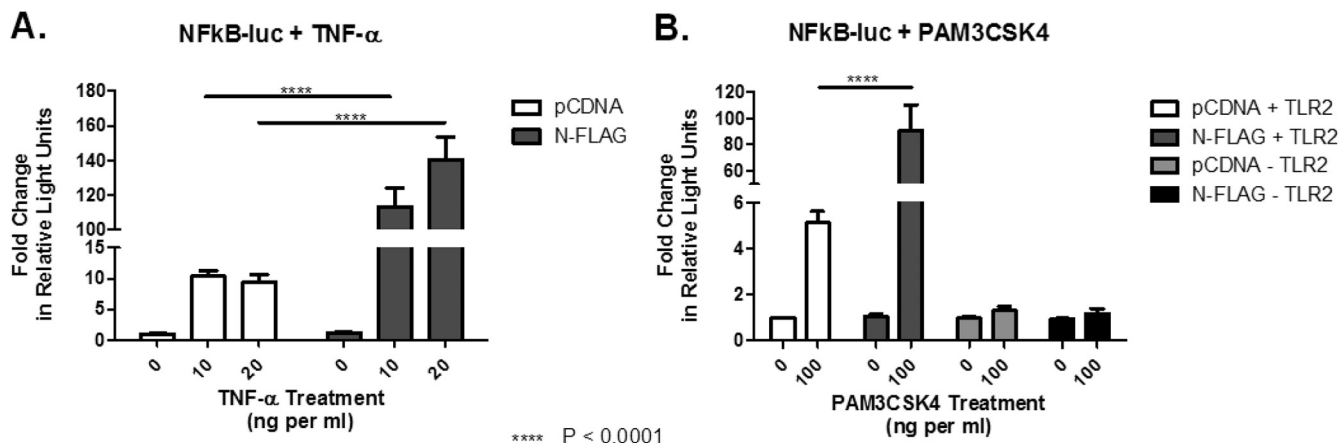
FIG 1 NF-κB activation is potentiated in the presence of OC43 N upon stimulation and is reflected in the cellular gene profile. (A) A luciferase reporter assay using a reporter vector (NF-κB-luc) with an NF-κB DNA-binding site promoter. Cells were stimulated with TNF-α for 24 h prior to measurement. All luciferase measurements were normalized to β-galactosidase. Data represent 8 independent experiments, each performed in duplicate. Error bars indicate standard errors of the means (SEM). (B) A TLR2-expressing plasmid was cotransfected with NF-κB-luc, and cells were stimulated with PAM3CSK4 for 24 h prior to measurement. Cells were also cotransfected with empty vector and NF-κB-luc to ensure any response seen was due to TLR2 signaling. All luciferase measurements were normalized to β-galactosidase. Data represent 2 independent experiments, each performed in triplicate. Error bars indicate SEM.

pression (26, 27). As with other protein regulators of NF-κB, the expression of miR-9 is inducible by stimuli which also activate NF-κB, such as TNF-α, LPS, and TLR2 agonists (26).

In the following, we report that HCoV OC43 N protein causes a potentiation of NF-κB activation when expressed *in vitro*. We also propose a novel mechanism by which this prolonged activation occurs where, due to its RNA-binding properties, OC43 N binds to negative regulator miR-9, allowing for NFKB1 translation. This previously undescribed interaction results in increased expression of NFKB1 products p105 and p50 in both transient-transfection and coronaviral infection scenarios.

MATERIALS AND METHODS

Cells and viruses. 293T cells were maintained in Dulbecco's modified Eagle's medium (DMEM) supplemented with 8% fetal calf serum (FCS), 2 mM L-glutamine, 100 U/ml penicillin, and 100 μg/ml streptomycin. HCT-8 cells (American Type Culture Collection [ATCC], Manassas, VA, USA) were maintained in RPMI supplemented with 8% FCS, 2 mM L-glutamine, 10 mM HEPES, 1 mM sodium pyruvate, 4.5 g/liter D-glucose, 1.5 g/liter sodium bicarbonate, 100 U/ml penicillin, and 100 μg/ml streptomycin. All cells were grown at 37°C in a 5% humidified CO_2 incubator. Matrix mutant ΔM51 vesicular stomatitis virus (VSV) expressing FLAG-tagged OC43 nucleocapsid protein (N-FLAG) was generated by PCR amplification of OC43 N with a FLAG sequence (DYKDDDDK) on the reverse primer, creating a C-terminal FLAG tag. Primer sequences were as follows: OC43 N Xho forward, 5′-GCCTCGAGGCCACCATGTCTTTTACTCCTGGTAAGCAAT-3′; OC43 N Xba reverse, 5′-GACACCTCAGAAATAGATTACAAGGATG ACGACGATAAGTAATCTAGAGC-3′. OC43 N-FLAG was subcloned into the Δ51 VSV genome between the G and L genes. The resulting virus genome was rescued and amplified in 293T cells. Coronavirus OC43 (ATCC VR-1558) was a kind gift from James Mahony. The virus was propagated in HCT-8 cells at 33°C for 3 days in serum-free RPMI. Supernatants and cell monolayers were collected and freeze-thawed. Cell debris was pelleted by centrifugation at 1,500 rpm for 10 min.

Plasmids. Coronaviral nucleocapsid (N) genes were amplified via RT-PCR using cDNA generated from coronavirus-infected cells. Primer sequences were as follows: OC43 N forward, 5′-GCCTCGAGGCCACCAT GTCTTTTACTCCTGGTAAGCAATCCA-3′; OC43 N reverse, 5′-CGAG ATCTTTACTTATCGTCGTCATCCTTGTAATCTATTTCTGAGGTGT CTTCATGATAGGGC-3′. The amplified genes were FLAG tagged and subcloned into expression vector pEF, which contains an elongation factor 1α promoter, via XhoI and BglII restriction sites. The plasmids containing β-galactosidase (β-Gal) and NF-κB-luc were kind gifts from Karen Mossman. pUNO-hTLR2 (Invivogen) was a kind gift from Dawn Bowdish. Empty vectors pCDNA3.1 (pCDNA) and pSG5 (Invitrogen and Agilent Technologies, respectively) were also utilized. The green fluorescent protein (GFP) expression plasmid, pEGFP-N1 (pEGFP), was also utilized (Clontech, Mountain View, CA, USA). The luciferase plasmid luc-NFKB1 was a kind gift from Massimo Locati. All plasmids were prepared with endotoxin-free kits (Qiagen).

Antibodies. Antibodies against FLAG were obtained from Rockland Immunochemicals Inc. (polyclonal) and Sigma-Aldrich (monoclonal) (Gilbertsville, PA, USA, and St. Louis, MO, USA, respectively). Antibodies against hnRNPU, Ku70, and nucleolin were also obtained from Santa Cruz Biotechnologies. Anti-YB1 was obtained from Cell Signaling (Danvers, MA, USA). Anti-β-actin was obtained from Sigma-Aldrich. Anti-NF-κBp50 was obtained from Santa Cruz Biotechnologies.

Luciferase reporter assay. 293T cells were plated in 24-well plates at a density of 1.3×10^5 cells per well. Cells were cotransfected with a luciferase reporter plasmid NF-κB-luc, β-Gal plasmid, and coronaviral N gene using Lipofectamine 2000 (Invitrogen). Cells were treated with TNF-α (10 or 20 ng/ml; Peprotech, Rocky Hill, NJ, USA) 24 h posttransfection. Twenty-four hours after treatment, cells were assayed for luciferase activity using the enhanced luciferase assay kit (BD Biosciences, Franklin Lakes, NJ, USA) and β-galactosidase activity using the luminescent β-Gal kit (Clontech). The TLR2 luciferase assay employed methods identical to those of the NF-κB-luc assay described above, with the exception that the TLR2 expression plasmid was also cotransfected with NF-κB-luc, β-Gal, and N gene plasmid. Cells were treated 24 h posttransfection with PAM3-CSK4 (100 ng/ml). Luciferase reporter assay for OC43 activation of NF-κB utilized HCT-8 cells cotransfected with luciferase reporter plasmid NF-κB-luc and β-Gal plasmid. Cells were infected with OC43 at a multiplicity of infection (MOI) of 1, 24 h posttransfection. Cells were lysed at 1, 2, and 3 days postinfection and assayed for luciferase activity as described above.

miR-targeted luciferase reporter assay. 293T cells were plated in 24-well plates at a density of 1.3×10^5 cells per well, and HEK293 cells were plated at a density of 5×10^4 in 24-well plates. Cells were cotransfected with a luciferase reporter plasmid, NFKB1-luc, OC43 N, or empty vector and miR mimic miR-9 (Sigma-Aldrich) using DharmaFECT Duo (Dhar-
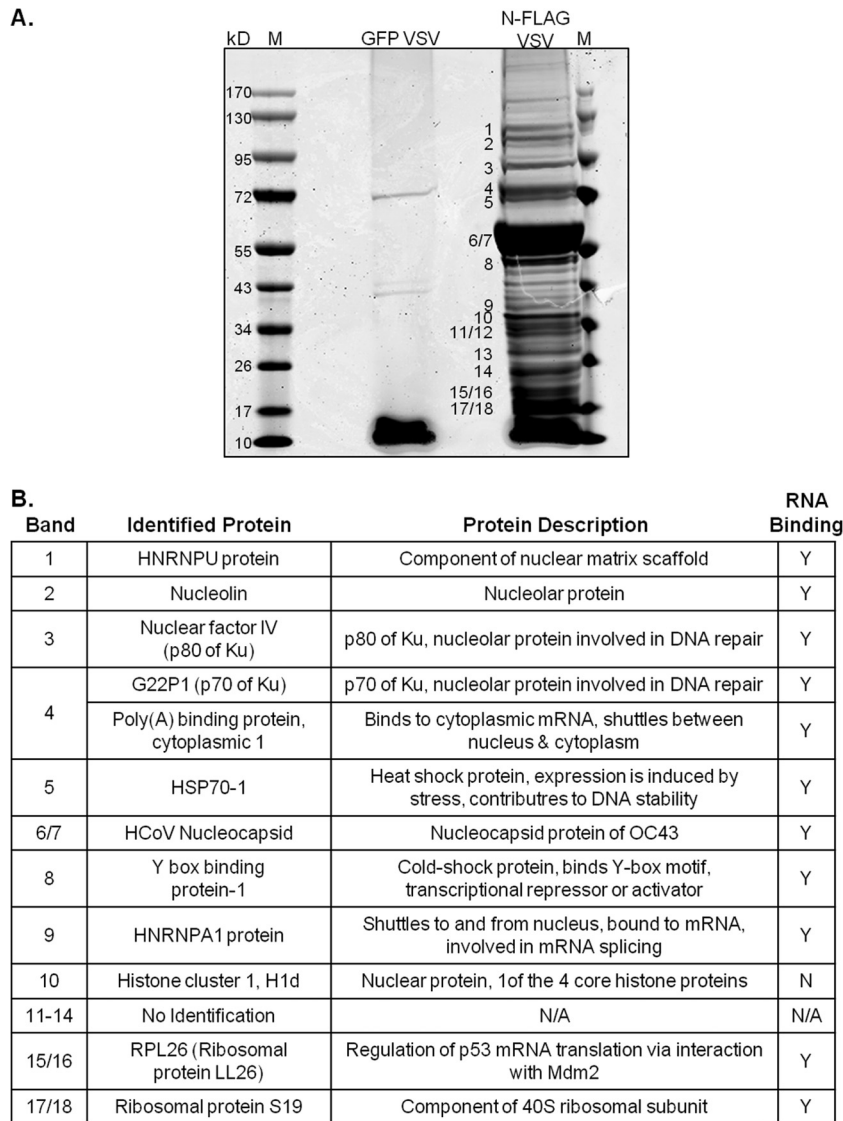
A.

B.

Band	Identified Protein	Protein Description	RNA Binding
1	HNRNPU protein	Component of nuclear matrix scaffold	Y
2	Nucleolin	Nucleolar protein	Y
3	Nuclear factor IV (p80 of Ku)	p80 of Ku, nucleolar protein involved in DNA repair	Y
4	G22P1 (p70 of Ku)	p70 of Ku, nucleolar protein involved in DNA repair	Y
	Poly(A) binding protein, cytoplasmic 1	Binds to cytoplasmic mRNA, shuttles between nucleus & cytoplasm	Y
5	HSP70-1	Heat shock protein, expression is induced by stress, contributres to DNA stability	Y
6/7	HCoV Nucleocapsid	Nucleocapsid protein of OC43	Y
8	Y box binding protein-1	Cold-shock protein, binds Y-box motif, transcriptional repressor or activator	Y
9	HNRNPA1 protein	Shuttles to and from nucleus, bound to mRNA, involved in mRNA splicing	Y
10	Histone cluster 1, H1d	Nuclear protein, 1of the 4 core histone proteins	N
11-14	No Identification	N/A	N/A
15/16	RPL26 (Ribosomal protein LL26)	Regulation of p53 mRNA translation via interaction with Mdm2	Y
17/18	Ribosomal protein S19	Component of 40S ribosomal subunit	Y

FIG 2 Proteins identified to coimmunoprecipitate with OC43 N. (A) Lysates of N-FL VSV and GFP VSV-infected cells were immunoprecipitated with an anti-FLAG antibody, and resulting precipitates were Coomassie stained. (B) Proteins coimmunoprecipitated with N-FL were identified by mass spectrometry. Numbered bands correspond with numbered bands in panel A.

macon, Lafayette, CO, USA). Cells were assayed for renilla and firefly luciferase 2 days posttransfection using the renilla luciferase assay system and the luciferase assay system (Promega, Madison, WI, USA).

Immunoprecipitation for protein interactions. FLAG-immunoprecipitation (IP) was carried out according to the manufacturer's protocols (Sigma). Briefly, 293T cells were plated in 150-cm dishes and infected with N-FLAG Δ51 VSV or GFP Δ51 VSV, each at an MOI of 5. Twenty-four hours postinfection (hpi), all cells were gathered and lysed in FLAG-IP lysis buffer with protease inhibitor (Roche). Lysates were incubated on ice for 30 min, and cell debris was spun out. The resulting supernatant was incubated overnight at 4°C with washed resin preconjugated with monoclonal FLAG antibody. The resulting resin was then washed, and precipitated proteins were eluted by competitive binding. The eluate was then concentrated via spin columns (Millipore). Eluate was run on precast SDS-PAGE gradient gels (Invitrogen) using the Novex midi-gel system (Invitrogen). Gels were stained for protein using Coomassie blue silver stain. Gels were scanned on the Odyssey imaging system (Licor). For RNase treatment, identical protocols were followed; however, prior to

incubation with FLAG resin, cell lysates were treated with RNase H (Thermo Scientific) or mock treated at 37°C.

Real-time PCR array. 293T cells were transfected with OC43 N-FLAG or pCDNA and subsequently treated with 10 ng/ml of TNF-α. RNA was extracted at 3 and 6 h posttreatment using the RT^2 quantitative PCR (qPCR)-Grade miRNA isolation kit (SABiosciences, Qiagen, Valencia, CA, USA). Reverse transcription of resulting RNA was performed using the RT^2 miRNA First Strand kit (SABiosciences). PCR arrays for human miRNome miRNA (MAH-100) (SABiosciences) were performed with RT^2 SYBR green qPCR master mix (SABiosciences) on the 7900HT real-time PCR system (Applied Biosystems).

RNA immunoprecipitation (RIP). 293T cells were either infected with N-FLAG (N-FL) VSV or GFP VSV or transfected with OC43 N-FL or pEGFP. Twenty-four hours postinfection or transfection, cells were lysed in FLAG-IP lysis buffer with protease inhibitor (Roche). The same immunoprecipitation procedure previously described using the commercial FLAG immunoprecipitation kit was followed. After elution, RNA was extracted from eluates using the miRNeasy minikit (Qiagen). Reverse
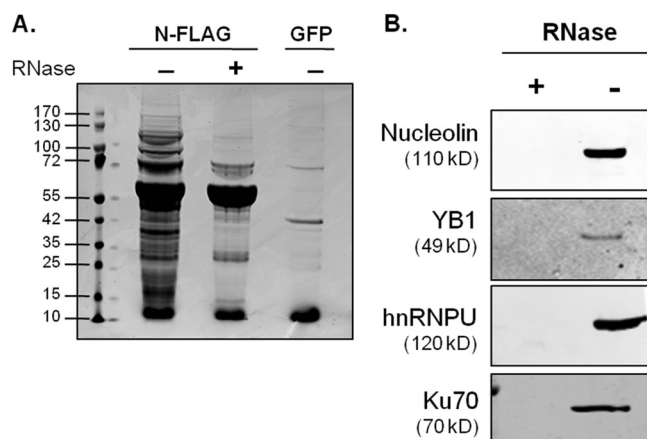
A.

B.

FIG 3 OC43 N interacts with many cellular proteins in an RNA-dependent manner. (A) Cell lysates of N-FL VSV-infected cells were treated with RNase or left untreated prior to FLAG immunoprecipitation. GFP VSV-infected cell lysates were again FLAG immunoprecipitated as a control. (B) Several proteins identified via mass spectrometry to interact with N-FL were confirmed to be pulled down with N. These interactions were eliminated when lysates were treated with RNase prior to immunoprecipitation.

transcription of resulting RNA was performed using the RT^2 miRNA First Strand kit (SABiosciences). qPCR was performed with commercial primers for miR-9 (SABiociences) and RT^2 SYBR green qPCR master mix (SABiosciences) on the 7900HT real-time PCR system (Applied Biosystems).

Flow cytometry. 293T cells were transfected with N-FLAG or pCDNA. Twenty-four hours posttransfection, cells were treated with 10 ng/ml of TNF-α for 6 h. Cells were then collected and fixed with Cytofix/Cytoperm fixation/permeabilization solution (BD Biosciences). Cells were costained with anti-NFKB1 (Santa Cruz) and anti-FLAG (Sigma) antibodies or anti-GFP as an isotype control. Subsequently, cells were stained with secondary antibodies, anti-rabbit 649 and anti-mouse 488. Cells were filtered, and flow cytometry was run on an LSR II (BD Biosciences).

RESULTS

The HCoV nucleocapsid potentiates NF-κB activation. Although the N proteins of SARS-CoV and fellow nidovirus porcine reproductive and respiratory syndrome virus have been demonstrated to effect NF-κB activation, the HCoV OC43 N protein has not been studied for its ability to alter NF-κB activation (16). In order to examine whether the N protein effected NF-κB activation, a plasmid expressing the nucleocapsid protein of OC43 was cotransfected into 293T cells with a luciferase reporter plasmid containing firefly luciferase under the control of an NF-κB DNA-binding domain. Unexpectedly, while expression of N protein alone failed to alter NF-κB activation, it was seen to cause a dramatic hyperactivation of NF-κB when cells were stimulated with tumor necrosis factor alpha (TNF-α), with luciferase levels measuring at least 10-fold higher than with TNF-α alone (Fig. 1A).

To determine if this phenomenon was TNF-α dependent, we sought to examine another pathway that initiates NF-κB activation. The Toll-like receptor 2 (TLR2) pathway is well characterized and activates NF-κB as a result of binding ligands such as Pam3CSK4, a synthetic lipoprotein. As 293T cells do not express TLR2, a plasmid containing TLR2 was also cotransfected in addition to N and NF-κB luciferase plasmids. Once again, inclusion of the N protein expression plasmid led to a greater-than-10-fold
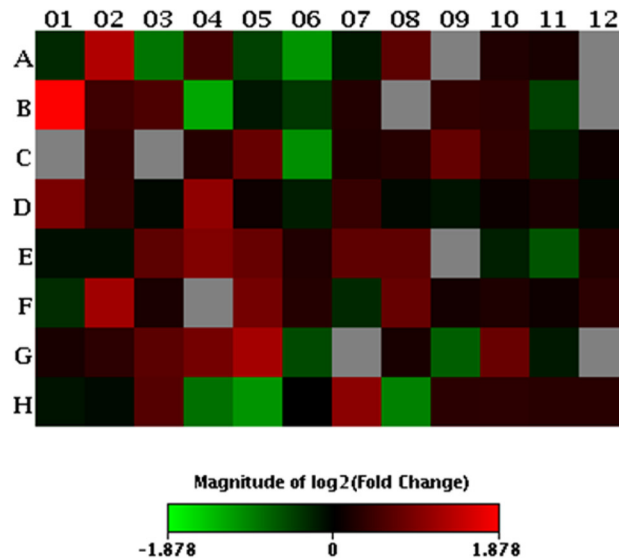
enhancement in the NF-κB response to stimulation (Fig. 1B). This signified that the phenomenon of potentiated NF-κB activation in the presence of OC43 N occurs via multiple pathways.

The discernment that the potentiation of NF-κB activation in N-transfected cells occurred only when a stimulus was applied led us to hypothesize that N may be affecting a negative regulator of NF-κB, thus preventing deactivation of the transcription factor. Therefore, the p65 subunit of NF-κB was examined for prolonged activation in the presence of OC43 N, which would point toward the malfunction of a p65-negative regulator. p65 nuclear localization, an indicator of activation, did not appear to endure longer in 293T cells expressing N after TNF-α stimulation, indicating that prolonged activation of this subunit was not responsible for the potentiation of NF-κB activation (data not shown). Additionally, the degradation kinetics of NF-κB inhibitor IκBα were examined via protein levels of IκBα in 293T cells after TNF-α treatment in the presence or absence of OC43 N. By Western blot analysis, the kinetics of IκBα degradation were indistinguishable between cells transfected with N and cells transfected with empty vector (data not shown). These data indicate that neither p65 activation nor IκBα degradation seem to be the point of interference by OC43 N.

OC43 nucleocapsid protein interacts with multiple cellular proteins in an RNA-dependent manner. Having eliminated p65 and its inhibitor IκBα as possible points of impact, we aimed to identify other interacting partners of OC43 N with the goal of discerning a negative regulator of NF-κB. In order to garner sufficient N protein expression, a vesicular stomatitis virus was generated expressing a FLAG-tagged N gene. A large number of 293T cells were infected with this virus, designated N-FLAG VSV, and control virus GFP VSV. Subsequent lysates were immunoprecipitated with an antibody against FLAG and run on gradient SDS-PAGE gels, and proteins coimmunoprecipitated with N were identified by mass spectrometry. A considerable number of cellular proteins were pulled down with N (Fig. 2A), and several unique bands were sequenced. Although no well-known NF-κB inhibitors were identified, it was confirmed that analogous to the majority of nidoviral nucleocapsid proteins examined, OC43 N interacts with the nucleolar protein nucleolin (Fig. 2B). Upon review, a trend emerged among the interacting proteins: virtually all possessed the ability to bind RNA.

As previously mentioned, N is a well-known RNA-binding protein which led us to inquire whether the interactions between N and the cellular proteins were direct or RNA dependent. To address this, cells were infected as before, and the lysates were treated with RNase prior to immunoprecipitation. Compared to untreated lysate, samples treated with RNase coimmunoprecipitated dramatically fewer proteins (Fig. 3A). Further, interactions with several cellular proteins that had been specifically confirmed by Western blot analysis were eliminated with RNase treatment (Fig. 3B).

OC43 N binds to miR-9, a negative inhibitor of NF-κB. The revelation that N was binding cellular proteins via RNA resulted in speculation that it may be binding or affecting functional, noncoding RNA species such as microRNA (miRNA). Initially, effects of N on cellular miRNAs were assessed by PCR array, allowing for 384 miRNAs to be screened. 293T cells were transfected with OC43 N or empty vector, followed by TNF-α stimulation. Although this assay did not indicate whether N was binding to cellular miRNAs, it revealed that the cellular miRNA expression pro-

FIG 4 Profiling of human miRNA expression indicates that OC43 N effects miR-9 levels. A heat map of a human miRNA PCR array comparing cells transfected with N-FLAG to pCDNA-transfected cells, both treated with TNF-α, shows various miR that are affected by N-FLAG. Of particular interest is hsa–miR-9 (B1), which is over 3-fold higher in N-FLAG cells than in pCDNA. Gray squares, unamplified.

	1	2	3	4	5	6	7	8	9	10	11	12
A	hsa-miR-142-5p **-1.23**	hsa-miR-16 **2.49**	hsa-miR-142-3p **-1.81**	hsa-miR-21 **1.41**	hsa-miR-15a **-1.39**	hsa-miR-29b **-2.15**	hsa-let-7a **-1.13**	hsa-miR-126 **1.59**	hsa-miR-143 **1.26**	hsa-let-7b **1.18**	hsa-miR-27a **1.13**	hsa-let-7f **1.26**
B	hsa-miR-9 **3.68**	hsa-miR-26a **1.38**	hsa-miR-24 **1.48**	hsa-miR-30e **-2.36**	hsa-miR-181a **-1.11**	hsa-miR-29a **-1.32**	hsa-miR-124 **1.19**	hsa-miR-144 **1.26**	hsa-miR-30d **1.28**	hsa-miR-19b **1.25**	hsa-miR-22 **-1.38**	hsa-miR-122 **1.26**
C	hsa-miR-150 **1.26**	hsa-miR-32 **1.29**	hsa-miR-155 **1.26**	hsa-miR-140-5p **1.21**	hsa-miR-125b **1.68**	hsa-miR-141 **-2.09**	hsa-miR-92a **1.17**	hsa-miR-424 **1.21**	hsa-miR-191 **1.67**	hsa-miR-17 **1.28**	hsa-miR-130a **-1.17**	hsa-miR-20a **1.08**
D	hsa-miR-27b **1.87**	hsa-miR-26b **1.3**	hsa-miR-146a **-1.04**	hsa-miR-200c **2.11**	hsa-miR-99a **1.07**	hsa-miR-19a **-1.16**	hsa-miR-23a **1.31**	hsa-miR-30a **-1.04**	hsa-let-7i **-1.1**	hsa-miR-93 **1.07**	hsa-let-7c **1.14**	hsa-miR-106b **-1.04**
E	hsa-miR-101 **-1.08**	hsa-let-7g **-1.07**	hsa-miR-425 **1.6**	hsa-miR-15b **1.93**	hsa-miR-28-5p **1.69**	hsa-miR-18a **1.17**	hsa-miR-25 **1.62**	hsa-miR-23b **1.61**	hsa-miR-302a **1.26**	hsa-miR-186 **-1.16**	hsa-miR-29c **-1.54**	hsa-miR-7 **1.19**
F	hsa-let-7d **-1.26**	hsa-miR-30c **2.28**	hsa-miR-181b **1.14**	hsa-miR-223 **1.26**	hsa-miR-320a **1.81**	hsa-miR-374a **1.21**	hsa-let-7e **-1.23**	hsa-miR-151-5p **1.68**	hsa-miR-374b **1.1**	hsa-miR-196b **1.17**	hsa-miR-140-3p **1.08**	hsa-miR-100 **1.26**
G	hsa-miR-103 **1.13**	hsa-miR-96 **1.25**	hsa-miR-302b **1.58**	hsa-miR-194 **1.81**	hsa-miR-125a-5p **2.33**	hsa-miR-423-5p **-1.46**	hsa-miR-376c **1.26**	hsa-miR-195 **1.13**	hsa-miR-222 **-1.62**	hsa-miR-28-3p **1.71**	hsa-miR-128 **-1.13**	hsa-miR-302c **1.26**
H	hsa-miR-423-3p **-1.1**	hsa-miR-185 **-1.05**	hsa-miR-30b **1.54**	hsa-miR-210 **-1.76**	SNORD48 **-2.15**	SNORD47 **-1**	SNORD44 **2.04**	RNU6-2 **-1.95**	miRTC **1.24**	miRTC **1.25**	PPC **1.23**	PPC **1.22**

file was altered by OC43 N. In the presence of N, a myriad of miRNA levels were altered, and miR-9 expression in particular showed over a 3-fold increase compared to that in the presence of empty vector (Fig. 4).

miR-9 targets *NFKB1*, which encodes the p105 and p50 subunits of NF-κB and is itself induced by NF-κB activation (26). We postulated that N could be functionally hindering the negative regulation of NFKB1 by interacting with miR-9. In order to test this theory, N was expressed in cells both by transfection and infection with N-FLAG VSV, nucleocapsid protein was immunoprecipitated, and the resulting immunoprecipitates were subjected to RNA extraction. miR-9 was detected by PCR in immunoprecipitates from cells expressing N but not the control plasmid (Fig. 5). This confirmed that OC43 N binds miR-9 and further supported the hypothesis that N was sequestering this negative regulator of NF-κB.

Elevated expression of NFKB1 occurs in OC43 N-expressing cells. We predicted that the prevention of miR-9's actions on

NFKB1 would lead to higher NFKB1 expression levels and next sought to determine the level of NFKB1 in cells expressing N. 293T cells transfected with N or empty vector were stimulated with TNF-α and lysed at various times poststimulation. Both p105 and p50 subunits were detected, quantified, and compared between samples. The total protein levels of NFKB1 were consistently higher in cells expressing N compared to empty vector (Fig. 6A).

To delineate NFKB1 levels in cells specifically expressing N, we examined cells via flow cytometry. This allowed for consideration of only those cells expressing N, as opposed to the entire population, which includes untransfected cells. Transfected 293T cells were stained with antibodies against FLAG and NFKB1. As is commonly found in transient transfection, N-transfected cells contained populations of cells with various levels of N expression. These two groups of cells were designated N_{hi} and N_{lo}, which expressed high levels and low levels of N protein, respectively (Fig. 6Bi). While cells expressing low levels of N did not display enhanced NFKB1 levels, those that strongly expressed N did, indi-
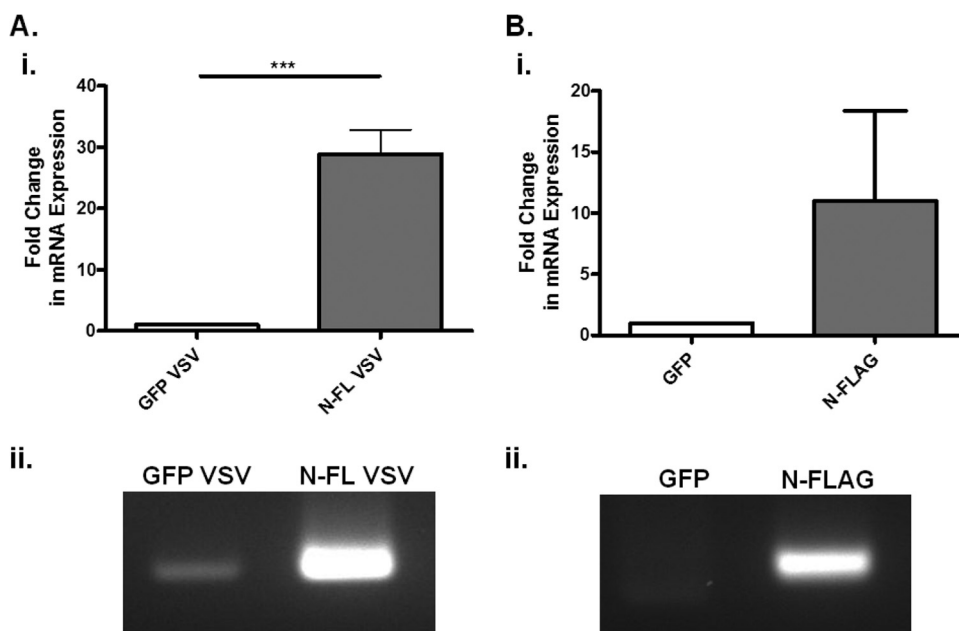
FIG 5 OC43 N interacts with miR-9. FLAG immunoprecipitation was performed on cells infected with N-FL VSV or GFP VSV (A) and transfected with N-FLAG or GFP (B). miR-9 was detected in N-containing immunoprecipitate by qRT-PCR (i) and also by conventional RT-PCR (ii).

cating that the steady-state level of NFKB1 correlated with N protein expression levels (Fig. 6Bii and iii). This verified the previous observation that in the cells expressing N, an elevated NFKB1 protein level is seen.

Sequestration of miR-9 by the N protein would be predicted to lead to increased levels of its target NFKB1 mRNA, leading to the increased steady-state levels of the NFKB1 protein described above. miR-9 is known to be NF-κB responsive, as it serves to provide negative feedback on NF-κB activity. Normally, NF-κB activation would increase miR-9 levels, which would serve to feed back on NFKB1 mRNA levels to negatively regulate the response; however, the presence of N protein may serve to prevent this function of miR-9, effectively blocking this negative feedback loop.

If N disrupted the regulation, it would be expected that an increase in NFKB1 mRNA could be observed. In addition, stimulation of the pathway with TNF-α, for example, would result in elevated transcription of NFKB1, and with the addition of N, a further amplification of NFKB1 mRNA would be observed. The mRNA levels of NFKB1 were investigated by qPCR in transfected and TNF-α-stimulated cells. NFKB1 mRNA in unstimulated N-transfected cells was slightly increased compared to that for the empty vector, though this difference was not statistically significant (Fig. 6C). In cells stimulated with TNF-α, however, the difference in NFKB1 mRNA between N- and empty vector-transfected cells was more pronounced (Fig. 6C).

OC43 N functionally impairs miR-9. Although it was ascertained that N both bound miR-9 and caused an increase in NFKB1 protein expression and mRNA, it remained to be determined whether N could affect miR-9 in a functional manner. A luciferase assay allowing for assessment of miR-9 function was utilized to establish whether N was preventing miR-9 from repressing translation of NFKB1. A luciferase expression construct containing the NFKB1 3′UTR (luc-NFKB1) was cotransfected into 293T cells with either N-FLAG or empty vector and with or without miR-9.

The endogenous miR-9 kept the constitutive expression of luciferase at a basal level, which was set to 1 for the purposes of comparison between experiments (Fig. 7). This suppression by endogenous miR-9 was prevented by the inclusion of N, as the levels of luciferase increased. As expected, the level of luciferase expression in empty vector-transfected cells was reduced with the addition of miR-9 (Fig. 7). Expression of N protein blocked the ability of the included exogenous miR-9 to suppress luciferase levels (Fig. 7). The differences observed with the addition of N were more pronounced in cells cotransfected with miR-9 compared to cells relying on endogenous miR-9, as it appears that expression levels of endogenous miR-9 in 293T cells are low.

N protein binds miR-9, and NFKB1 protein levels are elevated during OC43 infection. We sought to substantiate whether analogous phenomena could be observed in the context of a coronaviral infection. Initially, we investigated whether OC43 N bound miR-9 during a viral infection. HCT-8 cells were infected and lysed at 8 and 20 hpi. Immunoprecipitation with an antibody against OC43 N yielded immunoprecipitate from which RNA was extracted as described before. Quantitative PCR showed that as early as 8 hpi, N bound and pulled down miR-9 (Fig. 8A). The level of N protein expression was also assessed pre- and postimmunoprecipitation (whole-cell lysate and eluted protein, respectively), with N protein levels showing a marked increase from 8 hpi to 20 hpi (Fig. 8B).

HCT-8 cells were infected with OC43, and protein levels of NFKB1 were assessed via Western blot analysis at various times postinfection. As was observed in N-transfected cells, NFKB1 protein expression in OC43-infected cells was elevated compared to mock-infected cells (Fig. 9A and B). Similarly, by flow cytometry, OC43-infected cells also had increased levels of NFKB1 (Fig. 9C). This confirmed that NFKB1 protein expression was augmented in virally infected cells.

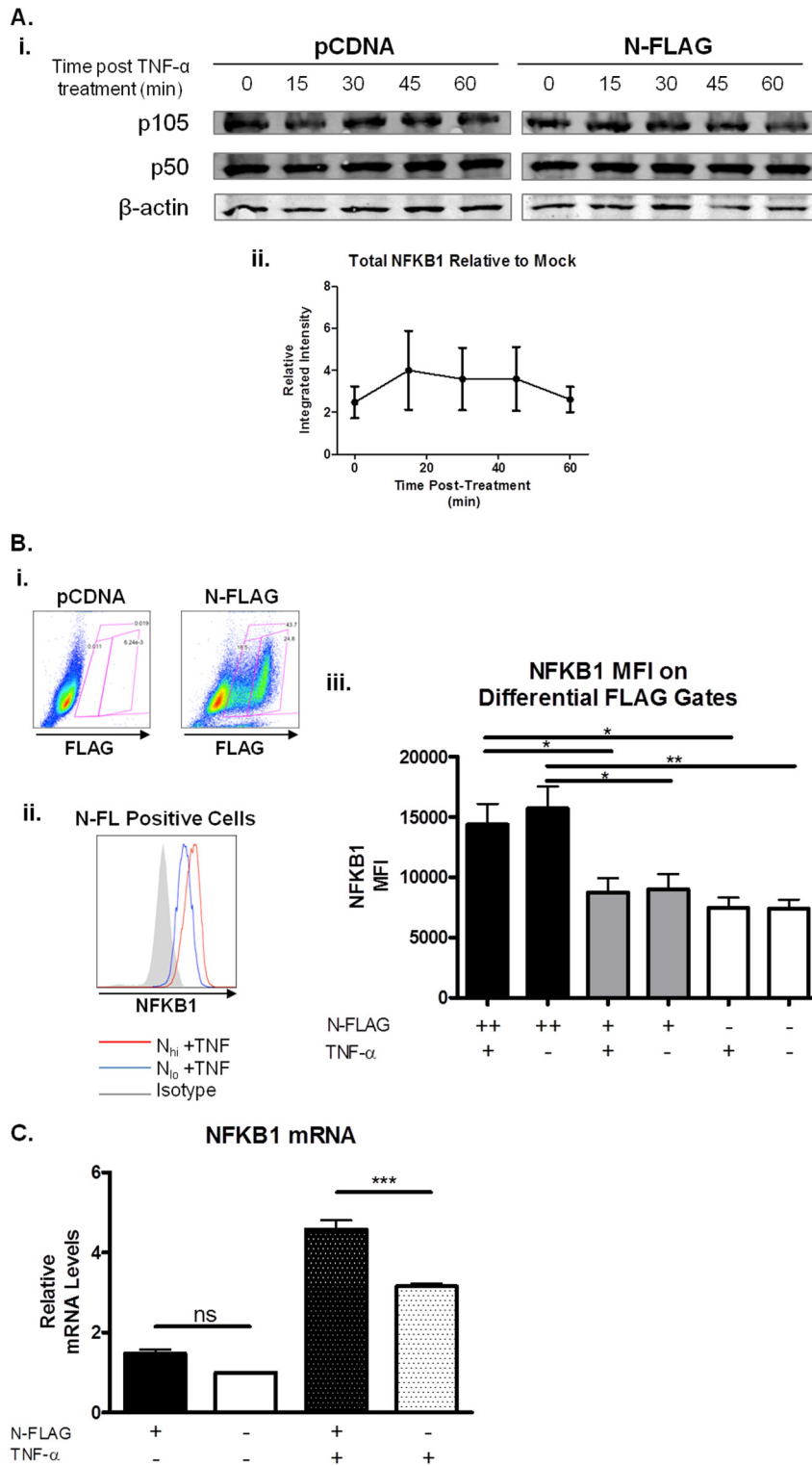Lastly, to assess whether OC43 activated NF-κB, HCT-8 cells

FIG 6 Presence of OC43 N results in elevated expression of NFKB1. (Ai) Western blot analysis detecting NFKB1 products p105 and p50 in cells transfected with pCDNA or N-FLAG and treated with TNF-α for various lengths of time. (ii) Quantification of the p105 and p50 bands shows that NFKB1 protein is more highly expressed in cells transfected with OC43 N. Values were normalized to β-actin. Data combined from 3 independent experiments. (B) Cells were transfected with N-FLAG or pCDNA and then treated with TNF-α or left untreated. Cells were then costained with antibodies against NFKB1 and FLAG, and protein expression was examined by flow cytometry. (i) FLAG staining specifically stained cells transfected with OC43 N. Two different populations of FLAG-positive cells were seen with various expression levels of FLAG, N_{hi} and N_{lo}. (ii) Comparison of NFKB1 levels in cells both positive for FLAG and NFKB1 show a difference in staining intensity between N_{hi} and N_{lo} cells. (iii) Graphical representation of mean fluorescent intensity of NFKB1 staining. In N_{hi} cells, the expression of NFKB1 is significantly higher than that of N_{lo} and pCDNA-transfected cells. Data combined from 2 independent experiments, performed in triplicate. (C) NFKB1 mRNA was detected by qRT-PCR in cells transfected with pCDNA or N-FLAG and either treated with TNF-α or left untreated. In cells transfected with OC43 N, NFKB1 mRNA levels were increased compared to those in pCDNA-transfected cells. All NFKB1 values were normalized to housekeeping gene GAPDH.
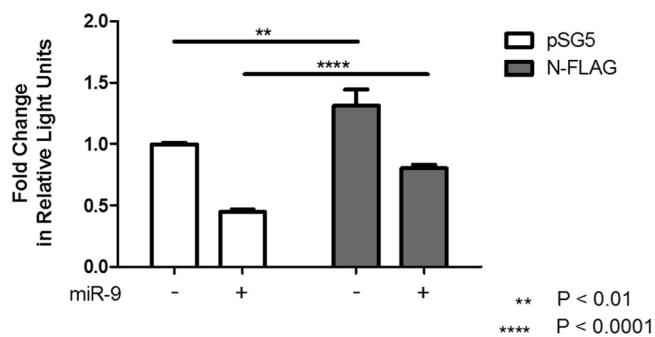
FIG 7 OC43 N prevents miR-9 negative regulation of NFKB1. The NFKB1 luciferase construct, luc-NFKB1, was cotransfected with either empty vector pSG5 or N-FLAG and with or without miR-9. When transfected with empty vector, a basal level of luciferase is observed. With the addition of miR-9, luciferase levels are reduced. The presence of N-FLAG blunts the effect of miR-9 on luciferase levels. All renilla luciferase measurements were normalized to firefly luciferase and subsequently compared to empty vector without miR-9. Data represent 3 independent experiments, each performed in triplicate.

were transfected with the NF-κB-luc construct and subsequently infected with OC43. At 1, 2, and 3 days postinfection, activation of NF-κB was higher in OC43-infected cells than in mock-infected cells (Fig. 10).

DISCUSSION

The findings of this study illustrate a novel method by which viruses can modify the host immune response. Although many viruses have been found to modulate signaling and subsequently activate NF-κB (reviewed in reference 28), human coronaviruses other than SARS-CoV have not been identified to interfere with this pathway. SARS-CoV membrane protein and papain-like protease (PLP) have been found to block NF-κB signaling, whereas the spike protein has been found to activate NF-κB (29–31). As aforementioned, one study reported that the N protein of SARS-CoV inhibited NF-κB activation via luciferase reporter assay (16), while others reported NF-κB activation by the nucleocapsid (14, 15). No mechanisms of interference were proposed in these reports.

We report here the unexpected observation that OC43 N protein expression significantly potentiates NF-κB activation follow-

ing cytokine or TLR ligand stimulation. Pursuit of the mechanism of the NF-κB activation potentiation eliminated any interference of OC43 N with the p65 subunit and its inhibitor IκBα. We did note, however, that the perpetuation of NF-κB activation by N occurred solely when the cells were stimulated. This indicated that the cell could not effectively turn off activated NF-κB when N was present and suggested that the point of interference was a negative regulator of NF-κB. We hypothesized that OC43 N was binding to a protein responsible for the negative regulation of NF-κB activation and sought to identify cellular proteins with which N interacted.

Many published studies have explored interactions between various nidovirus nucleocapsids and cellular proteins. It has been well established that there are many interactions with nuclear and nucleolar proteins, such as fibrillarin and nucleolin, though none have reported these interactions for OC43 N. Nor have any prior publications identified interacting partners directly involved in the regulation of NF-κB activation, and so we opted to investigate proteins that interacted with OC43 N. We identified numerous cellular proteins that interacted with N, among them nucleolin, and noted that the majority of them were RNA-binding proteins. The nucleocapsid itself is a known RNA-binding protein, as its main function in viral replication is to complex with the RNA genome (12). Taken together, this led to the suspicion that the identified protein interactions were indirect and RNA dependent. With RNase treatment, these interactions were revealed to be RNA dependent, which to our knowledge has not been previously recognized for other nidoviral nucleocapsid interactions, including the binding to nucleolin. This revelation gave rise to the prospect that the N protein could be binding to regulatory RNAs such as microRNAs. These small, noncoding RNAs have come to light as extremely important regulators of gene expression and play an essential role in the regulation of the innate immune response (reviewed in references 32, 33, and 34). Through a large genome-wide qPCR-based screen of miRNAs, we identified a multitude of miRNAs which were upregulated with OC43 N expression and TNF-α treatment. One of these miRNAs with increased expression that also had links to NF-κB was miR-9. Multiple studies, as well as predictive software, have implicated miR-9 in the prevention of NFKB1 translation by targeting the 3'UTR (26, 27, 35, 36).
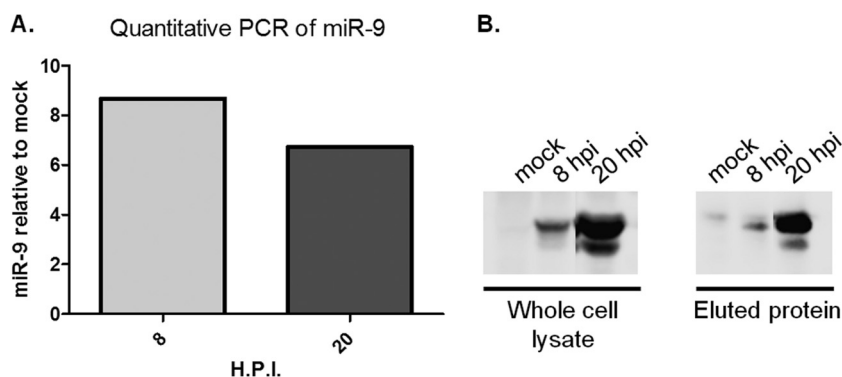

FIG 8 N interacts with miR-9 during OC43 infection. HCT-8 cells infected with OC43 were subjected to immunoprecipitation with antibody against N. (A) miR-9 was amplified by qPCR from RNA extracted from immunoprecipitates. Amplified miR-9 is expressed as fold change relative to mock-infected cells. Data are averaged from triplicates. Each sample was amplified in triplicate. (B) Representative portion of OC43 N expression at various time points during infection both from entire lysates preimmunoprecipitation (left) and immunoprecipitate (right).
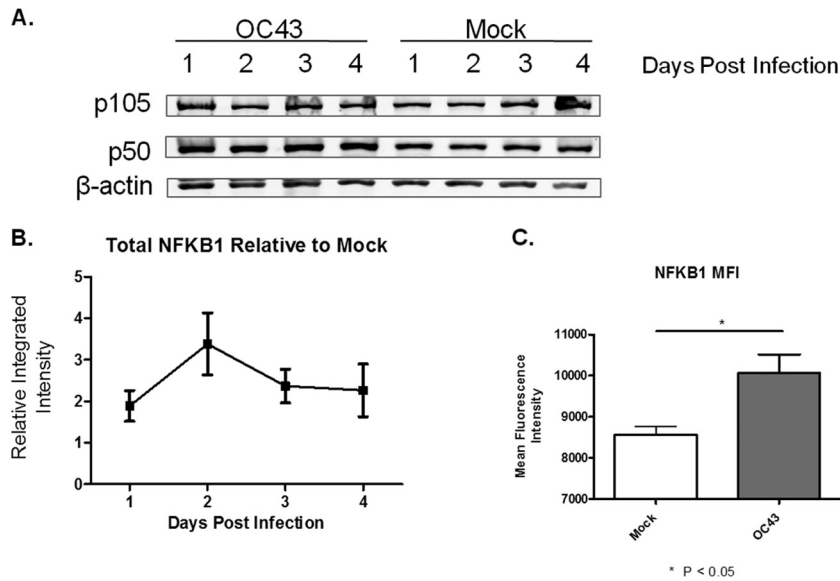
FIG 9 Infection with OC43 results in elevated expression of NFKB1. (A) Western blot analysis detecting NFKB1 products p105 and p50 in cells infected with OC43 for various lengths of time compared to uninfected cells. (B) Quantification of total NFKB1 in infected cells relative to mock-infected cells. All NFKB1 intensities were normalized to β-actin. Data combined from 3 independent experiments. (C) Flow cytometric analysis of OC43-infected cells compared to mock-infected cells at 1 day postinfection. Cells were costained with antibodies against NFKB1 and OC43 N protein. The mean fluorescence intensity of NFKB1 was significantly higher in infected cells than in mock-infected cells.

Additionally, miR-9 expression is inducible by TNF-α as well as by the TLR2 signaling pathways (26, 27).

We found that not only did the OC43 nucleocapsid bind miR-9, but it prevented its functionality via this interaction. When OC43 N was expressed in cells, elevated levels of both NFKB1 subunits were observed, demonstrating that the negative regulation of NFKB1 had been disrupted. The luciferase assay confirmed that N was functionally interfering with miR-9 function, as miR-9 suppression of luciferase via the NFKB1 3′UTR was reversed when N was present. In examining protein levels of NFKB1 via Western blot analysis and flow cytometry, cells treated with TNF-α did not show a significant difference in p105/p50 intensity compared to untreated cells. NFKB1 levels do not fluctuate greatly from basal

levels due to the tightly regulated expression of these proteins. This important negative feedback loop is significantly disrupted by the N protein, as observed by the increase in both steady-state and stimulated levels of NFKB1.

Similar interactions with miR-9 were seen in the context of an OC43 infection. We were able to coimmunoprecipitate and detect miR-9 with N from OC43-infected cells. The level of miR-9 detected at 20 hpi was lower than at 8 hpi, indicating a decreased associated of N with miR-9. This is juxtaposed with the level of N protein expression as detected by Western blot analysis (Fig. 8B). We speculate that N interacts more strongly with the viral genome, and as the infection progresses, increased binding of N to the OC43 genome is observed (data not shown), leading to a decrease in binding to miR-9. As expected with miR-9 sequestration, an increase in NFKB1 protein expression was seen in OC43-infected cells compared to that in mock-infected cells. Lastly, activation of NF-κB was also observed in OC43-infected cells via luciferase assay. These data combined support the hypothesis that during OC43 infection, the nucleocapsid protein binds miR-9 and prevents the negative regulation of NFKB1.

Taken together, our data have provided us with a hypothesized mechanistic model of how OC43 N is interacting with the NF-κB pathway. As seen in Fig. 11A, in resting, unstimulated cells, p105 is processed into p50, which then can homodimerize and act as a transcriptional repressor or activator depending on cofactors. p50 also dimerizes with other NF-κB members, such as p65, and remains in the cytoplasm in an inhibitory state. There is also a basal level of expression of NFKB1 mRNA and miR-9 in order to regulate NFKB1 translation. Upon stimulation, p50-p65 heterodimers are released from the control of IκBα and are able to translocate to the nucleus, where again, depending on whether they are bound to coactivators or corepressors, they activate or inhibit transcription (Fig. 11B). There is also a marked increase in NFKB1 mRNA and
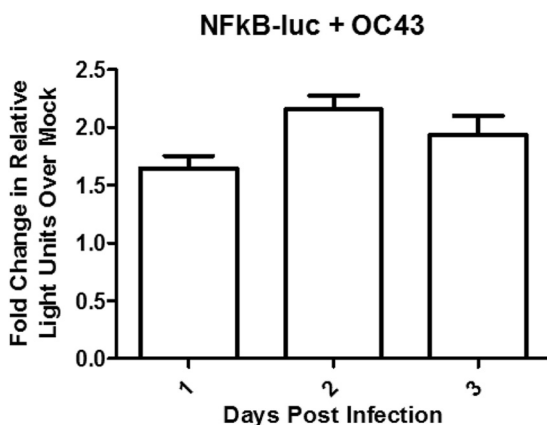

FIG 10 Infection with OC43 results in activation of NF-κB. HCT-8 cells were transfected with reporter plasmid NF-κB-luc and were subsequently infected with OC43. Measurement of luciferase at different days postinfection indicate activation of NF-κB. Data are represented as fold change over mock-infected cells.
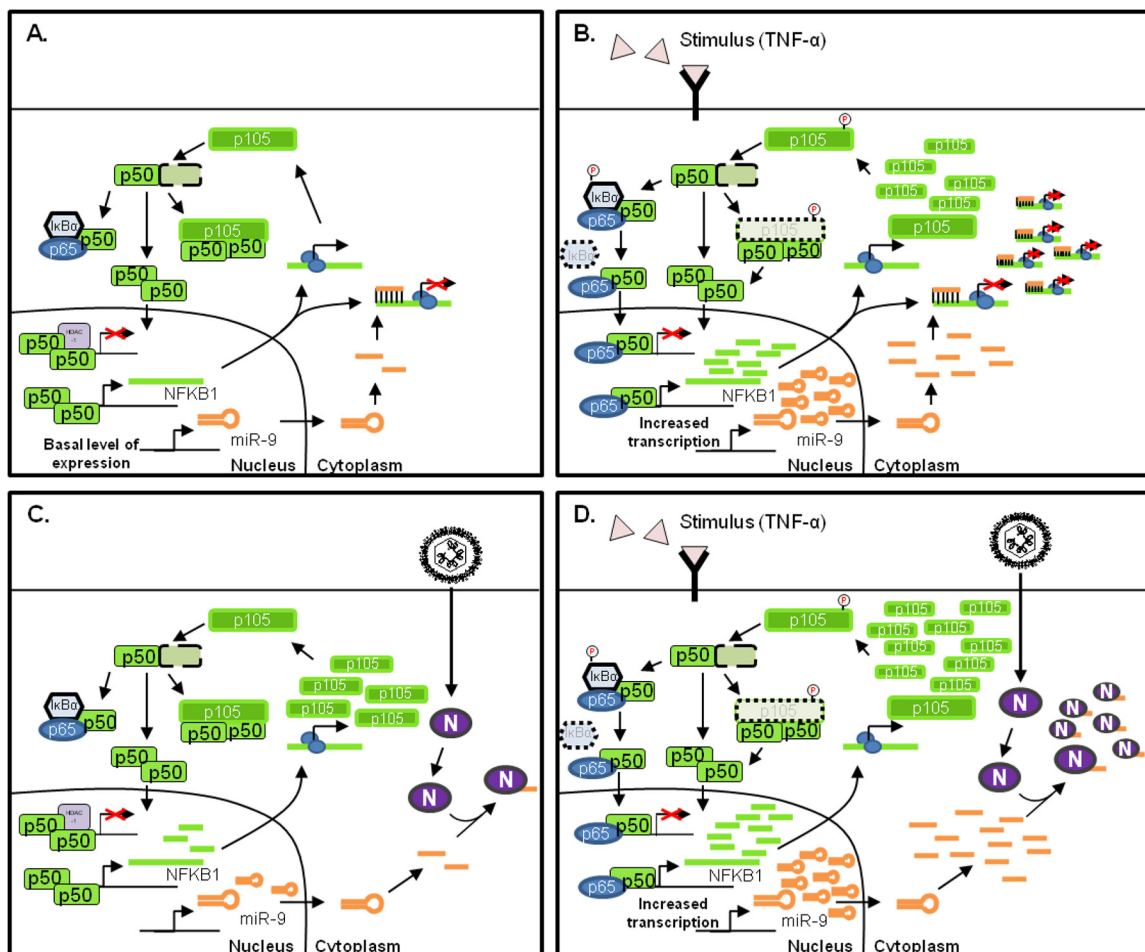
FIG 11 Proposed mechanism of HCoV N interference with NFKB1. (A) In resting cells, basal levels of NFKB1 and miR-9 are expressed. miR-9 negatively regulates NFKB1 expression. (B) With stimulus, a signaling cascade is initiated, resulting in increased transcription of both NFKB1 and miR-9. (C) Upon OC43 infection of cells, miR-9 is bound by the N protein, allowing for increased translation of NFKB1. (D) Addition of stimulus to OC43-infected cells further increases both NFKB1 and miR-9 transcription, but miR-9 is unable to act negatively in NFKB1 expression, as it is bound by OC43 N.

miR-9 upon stimulation. Figure 11C shows what we propose to be occurring when OC43 N is expressed in resting cells. OC43 N binds miR-9, which is basally expressed, and prevents its control of NFKB1 mRNA. With a stimulus such as TNF-α, both miR-9 and NFKB1 mRNA increase, but OC43 N continues to bind miR-9, preventing inhibition of NFKB1 translation (Fig. 11D). This interference in the negative-feedback mechanism of p105/ p50 expression leads to increased NFKB1 mRNA and therefore protein expression.

As to why OC43 potentiates NFKB1 activation, a few scenarios can be theorized. The first possibility is that this is merely an unintentional side effect of its RNA-binding nucleocapsid protein. In the context of an infection, there may be other viral proteins that aid in controlling the inflammatory response. As OC43 does not generally manifest in fatal infections, it is feasible that this is the key difference between OC43 and its fellow betacoronavirus, SARS-CoV. The latter causes immense levels of inflammation in the lungs of patients that does not resolve, resulting in high mortality. We also recognize that N is binding other miRNAs and mRNAs (data not shown) and that its interaction with cellular RNAs is not limited to miR-9, indicating that this contact may be

inadvertent. As N is an RNA-binding protein, it is not surprising that the N protein is able to associate with many different RNAs. The second possibility is that there is an advantage for OC43 to increase activated NFKB1. Although the subunit p50 can form dimers with other NF-κB subunits like p65, it may also form homodimers, and it can function as transcriptional repressors. The full-length subunit p105 is also an inhibitor of NF-κB subunits, and it can retain them in the cytoplasm. An excess of both of these subunits may lead to a state of repression for certain NF-κB targets, whereas normally in the context of a viral infection, a state of activation is desirable.

OC43 is by no means the only RNA virus with an RNA-binding protein, and this could be a common function across different genera of RNA viruses. Viruses such as influenza A, hepatitis C virus, and rubella virus all possess nucleocapsid proteins that complex with genomic RNA (37–39). Although several studies have shown that nucleocapsid recognizes viral RNA specifically, it is not necessarily surprising that a viral RNA-binding protein is able to bind cellular RNA (40, 41). miRNAs are an extremely important subset of cellular RNAs and have been the focus of a large volume of research since their discovery in the early 1990s (42).

Many groups have shown antiviral effects of miRNAs as well as viral manipulations of the miRNA pathways, including the encoding of viral miRNA mimics. This strategy is thought to be mainly a DNA virus specialty, as they typically have much larger genomes to encode extraneous virulence factors. RNA viruses must, as with other evasion tactics, be mutationally creative and utilize what little genomic space they possess. This often means multitasking of their encoded proteins. This novel mechanism of binding miRNAs to prevent function is a prime demonstration of how RNA viruses are constantly evolving to best the host immune system.

ACKNOWLEDGMENTS

REFERENCES

1. Ksiazek TG, Erdman D, Goldsmith CS, Zaki SR, Peret T, Emery S, Tong S, Urbani C, Comer JA, Lim W, Rollin PE, Dowell SF, Ling AE, Humphrey CD, Shieh WJ, Guarner J, Paddock CD, Rota P, Fields B, DeRisi J, Yang JY, Cox N, Hughes JM, LeDuc JW, Bellini WJ, Anderson LJ. 2003. A novel coronavirus associated with severe acute respiratory syndrome. N. Engl. J. Med. **348**:1953–1966. http://dx.doi.org/10.1056/NEJMoa030781.
2. McIntosh K, Becker WB, Chanock RM. 1967. Growth in suckling-mouse brain of "IBV-like" viruses from patients with upper respiratory tract disease. Proc. Natl. Acad. Sci. U. S. A. **58**:2268–2273. http://dx.doi.org/10.1073/pnas.58.6.2268.
3. Patrick DM, Petric M, Skowronski DM, Guasparini R, Booth TF, Krajden M, McGeer P, Bastien N, Gustafson L, Dubord J, Macdonald D, David ST, Srour LF, Parker R, Andonov A, Isaac-Renton J, Loewen N, McNabb G, McNabb A, Goh SH, Henwick S, Astell C, Guo JP, Drebot M, Tellier R, Plummer F, Brunham RC. 2006. An outbreak of human coronavirus OC43 infection and serological cross-reactivity with SARS coronavirus. Can. J. Infect. Dis. Med. Microbiol. **17**:330–336.
4. Vabret A, Mourez T, Gouarin S, Petitjean J, Freymuth F. 2003. An outbreak of coronavirus OC43 respiratory infection in Normandy, France. Clin. Infect. Dis. **36**:985–989. http://dx.doi.org/10.1086/374222.
5. Birch CJ, Clothier HJ, Seccull A, Tran T, Catton MC, Lambert SB, Druce JD. 2005. Human coronavirus OC43 causes influenza-like illness in residents and staff of aged-care facilities in Melbourne, Australia. Epidemiol. Infect. **133**:273–277. http://dx.doi.org/10.1017/S0950268804003346.
6. Hiscox JA, Wurm T, Wilson L, Britton P, Cavanagh D, Brooks G. 2001. The coronavirus infectious bronchitis virus nucleoprotein localizes to the nucleolus. J. Virol. **75**:506–512. http://dx.doi.org/10.1128/JVI.75.1.506-512.2001.
7. Wurm T, Chen H, Hodgson T, Britton P, Brooks G, Hiscox JA. 2001. Localization to the nucleolus is a common feature of coronavirus nucleoproteins, and the protein may disrupt host cell division. J. Virol. **75**:9345–9356. http://dx.doi.org/10.1128/JVI.75.19.9345-9356.2001.
8. Rowland RR, Kervin R, Kuckleburg C, Sperlich A, Benfield DA. 1999. The localization of porcine reproductive and respiratory syndrome virus nucleocapsid protein to the nucleolus of infected cells and identification of a potential nucleolar localization signal sequence. Virus Res. **64**:1–12. http://dx.doi.org/10.1016/S0168-1702(99)00048-9.
9. Chen H, Wurm T, Britton P, Brooks G, Hiscox JA. 2002. Interaction of the coronavirus nucleoprotein with nucleolar antigens and the host cell. J. Virol. **76**:5233–5250. http://dx.doi.org/10.1128/JVI.76.10.5233-5250.2002.
10. Zhao X, Nicholls JM, Chen YG. 2008. Severe acute respiratory syndrome-associated coronavirus nucleocapsid protein interacts with Smad3 and modulates transforming growth factor-beta signaling. J. Biol. Chem. **283**:3272–3280. http://dx.doi.org/10.1074/jbc.M708033200.
11. Luo C, Luo H, Zheng S, Gui C, Yue L, Yu C, Sun T, He P, Chen J, Shen J, Luo X, Li Y, Liu H, Bai D, Shen J, Yang Y, Li F, Zuo J, Hilgenfeld R, Pei G, Chen K, Shen X, Jiang H. 2004. Nucleocapsid protein of SARS coronavirus tightly binds to human cyclophilin A. Biochem. Biophys. Res. Commun. **321**:557–565. http://dx.doi.org/10.1016/j.bbrc.2004.07.003.
12. Zuniga S, Sola I, Moreno JL, Sabella P, Plana-Duran J, Enjuanes L.
2007. Coronavirus nucleocapsid protein is an RNA chaperone. Virology **357**:215–227. http://dx.doi.org/10.1016/j.virol.2006.07.046.
13. Zeng Y, Ye L, Zhu S, Zheng H, Zhao P, Cai W, Su L, She Y, Wu Z. 2008. The nucleocapsid protein of SARS-associated coronavirus inhibits B23 phosphorylation. Biochem. Biophys. Res. Commun. **369**:287–291. http://dx.doi.org/10.1016/j.bbrc.2008.01.096.
14. Zhang X, Wu K, Wang D, Yue X, Song D, Zhu Y, Wu J. 2007. Nucleocapsid protein of SARS-CoV activates interleukin-6 expression through cellular transcription factor NF-kappaB. Virology **365**:324–335. http://dx.doi.org/10.1016/j.virol.2007.04.009.
15. Liao QJ, Ye LB, Timani KA, Zeng YC, She YL, Ye L, Wu ZH. 2005. Activation of NF-kappaB by the full-length nucleocapsid protein of the SARS coronavirus. Acta Biochim. Biophys. Sin. **37**:607–612. http://dx.doi.org/10.1111/j.1745-7270.2005.00082.x.
16. Kopecky-Bromberg SA, Martinez-Sobrido L, Frieman M, Baric RA, Palese P. 2007. Severe acute respiratory syndrome coronavirus open reading frame (ORF) 3b, ORF 6, and nucleocapsid proteins function as interferon antagonists. J. Virol. **81**:548–557. http://dx.doi.org/10.1128/JVI.01782-06.
17. Hayden MS, Ghosh S. 2004. Signaling to NF-kappaB. Genes Dev. **18**:2195–2224. http://dx.doi.org/10.1101/gad.1228704.
18. Perkins ND. 2007. Integrating cell-signalling pathways with NF-kappaB and IKK function. Nat. Rev. Mol. Cell Biol. **8**:49–62. http://dx.doi.org/10.1038/nrm2083.
19. Moorthy AK, Savinova OV, Ho JQ, Wang VY, Vu D, Ghosh G. 2006. The 20S proteasome processes NF-kappaB1 p105 into p50 in a translation-independent manner. EMBO J. **25**:1945–1956. http://dx.doi.org/10.1038/sj.emboj.7601081.
20. Cohen S, Lahav-Baratz S, Ciechanover A. 2006. Two distinct ubiquitin-dependent mechanisms are involved in NF-kappaB p105 proteolysis. Biochem. Biophys. Res. Commun. **345**:7–13. http://dx.doi.org/10.1016/j.bbrc.2006.04.036.
21. Hoberg JE, Yeung F, Mayo MW. 2004. SMRT derepression by the IkappaB kinase alpha: a prerequisite to NF-kappaB transcription and survival. Mol. Cell **16**:245–255. http://dx.doi.org/10.1016/j.molcel.2004.10.010.
22. Watanabe N, Iwamura T, Shinoda T, Fujita T. 1997. Regulation of NFKB1 proteins by the candidate oncoprotein BCL-3: generation of NF-kappaB homodimers from the cytoplasmic pool of p50-p105 and nuclear translocation. EMBO J. **16**:3609–3620. http://dx.doi.org/10.1093/emboj/16.12.3609.
23. Motoyama M, Yamazaki S, Eto-Kimura A, Takeshige K, Muta T. 2005. Positive and negative regulation of nuclear factor-kappaB-mediated transcription by IkappaB-zeta, an inducible nuclear protein. J. Biol. Chem. **280**:7444–7451. http://dx.doi.org/10.1074/jbc.M412738200.
24. Huang WC, Ju TK, Hung MC, Chen CC. 2007. Phosphorylation of CBP by IKKalpha promotes cell growth by switching the binding preference of CBP from p53 to NF-kappaB. Mol. Cell **26**:75–87. http://dx.doi.org/10.1016/j.molcel.2007.02.019.
25. Werner SL, Kearns JD, Zadorozhnaya V, Lynch C, O'Dea E, Boldin MP, Ma A, Baltimore D, Hoffmann A. 2008. Encoding NF-kappaB temporal control in response to TNF: distinct roles for the negative regulators IkappaBalpha and A20. Genes Dev. **22**:2093–2101. http://dx.doi.org/10.1101/gad.1680708.
26. Bazzoni F, Rossato M, Fabbri M, Gaudiosi D, Mirolo M, Mori L, Tamassia N, Mantovani A, Cassatella MA, Locati M. 2009. Induction and regulatory function of miR-9 in human monocytes and neutrophils exposed to proinflammatory signals. Proc. Natl. Acad. Sci. U. S. A. **106**:5282–5287. http://dx.doi.org/10.1073/pnas.0810909106.
27. Guo LM, Pu Y, Han Z, Liu T, Li YX, Liu M, Li X, Tang H. 2009. MicroRNA-9 inhibits ovarian cancer cell growth through regulation of NF-kappaB1. FEBS J. **276**:5537–5546. http://dx.doi.org/10.1111/j.1742-4658.2009.07237.x.
28. Rahman MM, McFadden G. 2011. Modulation of NF-kappaB signalling by microbial pathogens. Nat. Rev. Microbiol. **9**:291–306. http://dx.doi.org/10.1038/nrmicro2539.
29. Frieman M, Ratia K, Johnston RE, Mesecar AD, Baric RS. 2009. Severe acute respiratory syndrome coronavirus papain-like protease ubiquitin-like domain and catalytic domain regulate antagonism of IRF3 and NF-kappaB signaling. J. Virol. **83**:6689–6705. http://dx.doi.org/10.1128/JVI.02220-08.
30. Dosch SF, Mahajan SD, Collins AR. 2009. SARS coronavirus spike protein-induced innate immune response occurs via activation of the NF-

kappaB pathway in human monocyte macrophages in vitro. Virus Res. **142:**19–27. http://dx.doi.org/10.1016/j.virusres.2009.01.005.

31. **Fang X, Gao J, Zheng H, Li B, Kong L, Zhang Y, Wang W, Zeng Y, Ye L.** 2007. The membrane protein of SARS-CoV suppresses NF-kappaB activation. J. Med. Virol. **79:**1431–1439. http://dx.doi.org/10.1002/jmv.20953.

32. **Gantier MP.** 2010. New perspectives in MicroRNA regulation of innate immunity. J. Interferon Cytokine Res. **30:**283–289. http://dx.doi.org/10.1089/jir.2010.0037.

33. **O'Neill LA, Sheedy FJ, McCoy CE.** 2011. MicroRNAs: the fine-tuners of Toll-like receptor signalling. Nat. Rev. Immunol. **11:**163–175. http://dx.doi.org/10.1038/nri2957.

34. **Ambros V.** 2004. The functions of animal microRNAs. Nature **431:**350–355. http://dx.doi.org/10.1038/nature02871.

35. **Arora H, Qureshi R, Jin S, Park AK, Park WY.** 2011. miR-9 and let-7g enhance the sensitivity to ionizing radiation by suppression of NFkappaB1. Exp. Mol. Med. **43:**298–304. http://dx.doi.org/10.3858/emm.2011.43.5.031.

36. **Wan HY, Guo LM, Liu T, Liu M, Li X, Tang H.** 2010. Regulation of the transcription factor NF-kappaB1 by microRNA-9 in human gastric adenocarcinoma. Mol. Cancer **9:**16. http://dx.doi.org/10.1186/1476-4598-9-16.

37. **Law LMJ, Everitt JC, Beatch MD, Holmes CFB, Hobman TC.** 2003. Phosphorylation of rubella virus capsid regulates its RNA binding activity and virus replication. J. Virol. **77:**1764–1771. http://dx.doi.org/10.1128/JVI.77.3.1764-1771.2003.

38. **Ye Q, Krug RM, Tao YJ.** 2006. The mechanism by which influenza A virus nucleoprotein forms oligomers and binds RNA. Nature **444:**1078–1082. http://dx.doi.org/10.1038/nature05379.

39. **Santolini E, Migliaccio G, La Monica N.** 1994. Biosynthesis and biochemical properties of the hepatitis C virus core protein. J. Virol. **68:**3631–3641.

40. **Chen H, Gill A, Dove BK, Emmett SR, Kemp CF, Ritchie MA, Dee M, Hiscox JA.** 2005. Mass spectroscopic characterization of the coronavirus infectious bronchitis virus nucleoprotein and elucidation of the role of phosphorylation in RNA binding by using surface plasmon resonance. J. Virol. **79:**1164–1179. http://dx.doi.org/10.1128/JVI.79.2.1164-1179.2005.

41. **Stohlman SA, Baric RS, Nelson GN, Soe LH, Welter LM, Deans RJ.** 1988. Specific interaction between coronavirus leader RNA and nucleocapsid protein. J. Virol. **62:**4288–4295.

42. **Lee RC, Feinbaum RL, Ambros V.** 1993. The C. elegans heterochronic gene lin-4 encodes small RNAs with antisense complementarity to lin-14. Cell **75:**843–854. http://dx.doi.org/10.1016/0092-8674(93)90529-Y.